

Fig. 6. (A) A comparison of calculated CBF images obtained by PET (top two) and SPECT (bottom two) from a typical clinical study with the rest-acetazolamide protocol. CBF images are shown for both first (first and third rows) and second (second and fourth rows) scans, respectively, and reveal that the present method is comparable with that by PET in CBF estimation. CBF images obtained by the present method (bottom two) were also compared with those (top two) by the conventional H₂¹⁵O ARG PET. All images are displayed with the same color scale in units of ml/100 g/min. (B) Comparison of calculated CBF values obtained from the rest-acetazolamide studies with dual-headed camera and PET ($n=6$). Each value corresponds to a mean value of regions of interest in each area of deep and cortical gray matter (frontal, temporal, occipital gyri) and cerebellum. (C) Comparison of %increase of CBF values calculated with the CBF values of (B). %increase of CBF was calculated by $[(\text{CBF}(\text{acetazolamide})/\text{CBF}(\text{rest})) - 1] \times 100$.

restricted by this limitation. It is, however, important to note that the CBF estimated by the present method was highly weighted by the transient CBF for a certain period. This contribution of

transient weight in the estimated CBF has been discussed already in previous publications for H₂¹⁵O PET ARG (Iida et al., 1991), and this has been applied to cognitive activation studies to detect 30-s

momentary change (Silbersweig et al., 1993, 1994). All of these findings support the validity of the present Dual-Table ARG approach for estimating CBF maps with the split-dose administration of IMP.

The evaluation of rest-acetazolamide CBF was a goal of the application of this methodology. This is based on the on-going project in Japan, which re-evaluates the previous reports regarding the value of extracranial/intracranial arterial anastomosis in patients with symptomatic occlusive disease of the internal carotid artery (Vorstrup et al., 1984; The-EC IC-Bypass-Study-Group, 1985a,b; Vorstrup et al., 1986). The previous study failed to show significant efficacy of the bypass surgery, but it did not selected patients by the aid of information for cerebral hemodynamics using functional imaging. The on-going project is intended to select only the severely ischemic patients (Stage II ischemia) by means of evaluating the reduced baseline CBF with a lack of vasoreactivity after acetazolamide challenge (Powers, 1991; Hayashida et al., 1996, 1999). PET is able to provide useful information (Powers and Raichle, 1985), but due to its limited availability in clinical centers, this Dual-Table ARG approach with IMP and SPECT may be of use for this project. A further evaluation is needed to confirm this.

The present Dual-Table ARG method may be applied to other tracer studies. Chmielowska et al. (1998, 1999) claimed that the qualitative CBF mapping during cognitive activation may be obtained with a 6-min interval by involving a simple background subtraction, yielding consistent activation foci as compared with a traditional protocol based on repeat PET scanning with repeat $H_2^{15}O$ injection at 10- to 12-min interval. DT-ARG approach to various tracer studies was evaluated by simulation (Iida et al., 2000), in which dual bolus administration and transient CBF change were simulated with assumption of $V_d=28$ for IMP and $V_d=0.8$ for $H_2^{15}O$, respectively. The simulation demonstrated that the increased CBF is estimated only when the true CBF was increase at the extremely early phase after the administration of IMP or $H_2^{15}O$, while the second CBF was independent of the change of CBF during previous scans in the both IMP and $H_2^{15}O$ simulations. Application of the present Dual-Table ARG approach to the $H_2^{15}O$ PET activation study may be able to further shorten the scan interval (approximately 1.5 min) (Watabe et al., 2002), by incorporating the background radioactivity distribution into the kinetic model formulation. Another possibility is the quantitative $CMRO_2$ study by means of PET scans following sequential administration of $^{15}O_2$ and $H_2^{15}O$. The previous protocol proposed by Mintun et al. (1984) was based on independent three step measurements following each of the $C^{15}O$, $^{15}O_2$ and $H_2^{15}O$ administration. The present approach, with the help of the estimated background radioactivity distribution in the sequential administration, could reduce the intervals between the scans without the loss of quantitative accuracy and image quality of each functional images of $CMRO_2$ and CBF, respectively, in anesthetized monkey study (Kudomi et al., 2005). Systematic studies are obviously needed in order to evaluate the feasibility of this technique in clinical studies.

We have previously demonstrated the importance of accurate image reconstruction in SPECT and employed a novel program package in order to achieve accurate reconstruction. Scatter, which was shown to cause serious reduction of the image contrast between the high CBF and low CBF areas, was corrected by the previously validated TDCS method (Meikle et al., 1994; Narita et al., 1996; Iida et al., 1998) together with correction for the penetration from the high-energy contaminations

(Kim et al., 2001). The photon attenuation correction was included in the OS-EM reconstruction procedure by using the attenuation map that was estimated from the head contour of its own MRI image (Iida et al., 1998). Details of the procedures and their validation have been described elsewhere (Iida et al., 1998; Kim et al., 2001). These procedures improved image contrast, and enabled to provide quantitative image that are equivalent to PET ($y(\text{ml}/100 \text{ g min})=1.07 \times (\text{ml}/100 \text{ g min})-1.14$, $r=0.94$).

In conclusion, CBF can be quantified by means of split-dose administration of IMP using SPECT. Contribution of the background radioactivity attributed to the previous administration of radiotracer can be built into the model, with minimal enhancement of statistical noise. The estimated CBF appeared to be most sensitive to the transient CBF immediately after the IMP injection but not to later periods, thus allowing the pharmacological challenges even during the first SPECT scan. Repeat quantitation of CBF could be feasible with considerably shorter intervals than with previous approaches. Accuracy of this approach was sufficiently high and may be of use for clinical studies.

Acknowledgment

This study was supported by the Program for Promotion of Fundamental Studies in Health Science of the Organization for Pharmaceutical Safety and Research (of Japan).

References

- Chmielowska, J., Coghill, R.C., Maisog, J.M., Carson, R.E., Herscovitch, P., Honda, M., Chen, R., Hallett, M., 1998. Positron emission tomography [^{15}O]water studies with short interscan interval for single-subject and group analysis: influence of background subtraction. *J. Cereb. Blood Flow Metab.* 18, 433–443.
- Chmielowska, J., Coghill, R.C., Carson, R.E., Ishii, K., Chen, R., Hallett, M., Herscovitch, P., 1999. Comparison of PET [^{15}O] water studies with 6-minute and 10-minute interscan intervals: single-subject and group analyses. *J. Cereb. Blood Flow Metab.* 19, 570–582.
- Hashikawa, K., Matsumoto, M., Moriwaki, H., Oku, N., Okazaki, Y., Uehara, T., Handa, N., Kusuoka, H., Kamada, T., Nishimura, T., 1994. Split dose iodine-123-IMP SPECT: sequential quantitative regional cerebral blood flow change with pharmacological intervention. *J. Nucl. Med.* 35, 1226–1233.
- Hatazawa, J., Iida, H., Shimosegawa, E., Sato, T., Murakami, M., Miura, Y., 1997. Regional cerebral blood flow measurement with iodine-123-IMP autoradiography: normal values, reproducibility and sensitivity to hypoperfusion. *J. Nucl. Med.* 38, 1102–1108.
- Hattori, N., Yonekura, Y., Tanaka, F., Fujita, T., Wang, J., Ishizu, K., Okazawa, H., Tamaki, N., Konishi, J., 1996. One-day protocol for cerebral perfusion reserve with acetazolamide. *J. Nucl. Med.* 37, 2057–2061.
- Hayashida, K., Tanaka, Y., Hirose, Y., Kume, N., Iwama, T., Miyake, Y., Ishida, Y., Matsuura, H., Miyake, Y., Nishimura, T., 1996. Vasoreactive effect of acetazolamide as a function of time with sequential PET ^{15}O -water measurement. *Nucl. Med. Commun.* 17, 1047–1051.
- Hayashida, K., Fukuchi, K., Hasegawa, Y., Kume, N., Cho, I.H., Nishimura, T., 1999. Viable tissue in an area of severely reduced perfusion demonstrated with I-123 iomazenil brain SPECT imaging of benzodiazepine receptors. *Clin. Nucl. Med.* 24, 576–578.
- Hudson, H.M., Iarkin, R.S., 1994. Accelerated image reconstruction using ordered subsets of projection data. *IEEE Trans. Med. Imaging* 13, 601–609.

- Iida, H., Kanno, I., Miura, S., Murakami, M., Takahashi, K., Uemura, K., 1986. Error analysis of a quantitative cerebral blood flow measurement using $H_2^{18}O$ autoradiography and positron emission tomography, with respect to the dispersion of the input function. *J. Cereb. Blood Flow Metab.* 6, 536–545.
- Iida, H., Higano, S., Tomura, N., Shishido, F., Kanno, I., Miura, S., Murakami, M., Takahashi, K., Sasaki, H., Uemura, K., 1988. Evaluation of regional differences of tracer appearance time in cerebral tissues using [^{15}O] water and dynamic positron emission tomography. *J. Cereb. Blood Flow Metab.* 8, 285–288.
- Iida, H., Kanno, I., Miura, S., Murakami, M., Takahashi, K., Uemura, K., 1989. A determination of the regional brain/blood partition coefficient of water using dynamic positron emission tomography. *J. Cereb. Blood Flow Metab.* 9, 874–885.
- Iida, H., Kanno, I., Miura, S. (Eds.), 1991. Rapid Measurement of Cerebral Blood Flow with Positron Emission Tomography. Exploring the Brain Functional Anatomy with Positron Tomography. John Wiley & Sons, Chichester.
- Iida, H., Itoh, H., Bloomfield, P.M., Munaka, M., Higano, S., Murakami, M., Inugami, A., Eberl, S., Aizawa, Y., Kanno, I., Uemura, K., 1994a. A method to quantitate cerebral blood flow using a rotating gamma camera and iodine-123 iodoamphetamine with one blood sampling. *Eur. J. Nucl. Med. Mol. Imaging* 21, 1072–1084.
- Iida, H., Itoh, H., Nakazawa, M., Hatazawa, J., Nishimura, H., Onishi, Y., Uemura, K., 1994b. Quantitative mapping of regional cerebral blood flow using iodine-123-IMP and SPECT. *J. Nucl. Med.* 35, 2019–2030.
- Iida, H., Akutsu, T., Endo, K., Fukuda, H., Inoue, T., Ito, H., Koga, S., Komatani, A., Kuvabara, Y., Momose, T., Nishizawa, S., Odano, I., Ohkubo, M., Sasaki, Y., Suzuki, H., Tanada, S., Toyama, H., Yonekura, Y., Yoshida, T., Uemura, K., 1996. A multicenter validation of regional cerebral blood flow quantitation using [^{123}I]iodoamphetamine and single photon emission computed tomography. *J. Cereb. Blood Flow Metab.* 16, 781–793.
- Iida, H., Narita, Y., Kado, H., Kashikura, A., Sugawara, S., Shoji, Y., Kinoshita, T., Ogawa, T., Eberl, S., 1998. Effects of scatter and attenuation correction on quantitative assessment of regional cerebral blood flow with SPECT. *J. Nucl. Med.* 39, 181–189.
- Iida, H., Watabe, H., Shidahara, M., Kim, K.M., Ogura, T., 2000. Modeling strategy for background compensation in repeat cerebral blood flow quantitation with diffusible tracers. *IEEE Med. Conf. Proc.* 2, 34–39.
- Imaizumi, M., Kitagawa, K., Hashikawa, K., Oku, N., Teratani, T., Takasawa, M., Yoshikawa, T., Rishu, P., Ohtsuki, T., Hori, M., Matsumoto, M., Nishimura, T., 2002. Detection of misery perfusion with split-dose [^{123}I]iodoamphetamine single-photon emission computed tomography in patients with carotid occlusive diseases. *Stroke* 33, 2217–2223.
- Kanno, I., Iida, H., Miura, S., Murakami, M., Takahashi, K., Sasaki, H., Inugami, A., Shishido, F., Uemura, K., 1987. A system for cerebral blood flow measurement using an $H_2^{18}O$ autoradiographic method and positron emission tomography. *J. Cereb. Blood Flow Metab.* 7, 143–153.
- Kim, K.M., Watabe, H., Shidahara, M., Ishida, Y., Iida, H., 2001. SPECT collimator dependency of scatter and validation of transmission dependent scatter compensation methodologies. *IEEE Trans. Nucl. Sci.* 48, 689–696.
- Kudomi, N., Hayashi, T., Teramoto, N., Watabe, H., Kawachi, N., Ohta, Y., Kim, K.M., Iida, H., 2005. Rapid quantitative measurement of CMRO₂ and CBF with the dual administration of ^{15}O -labeled oxygen and water during a single PET scan—A validation study with error analysis in anesthetized monkeys. *J. Cereb. Blood Flow Metab.* 25, 1209–1224.
- Kuhl, D.E., Barrio, J.R., Huang, S.C., Selin, C., Ackermann, R.F., Lear, J.L., Wu, J.L., Lin, T.H., Phelps, M.E., 1982. Quantifying local cerebral blood flow by *N*-isopropyl- μ -[^{123}I]iodoamphetamine (IMP) tomography. *J. Nucl. Med.* 23, 196–203.
- Kurusu, R., Ogura, T., Takikawa, S., Saito, H., Nakazawa, M., Iida, H., 2002. Estimation and optimization of the use of standard arterial input function for split-dose administration of *N*-isopropyl- μ -[^{123}I]iodoamphetamine. *Kaku Igaku* 39, 13–20.
- Lear, J.L., Ackermann, R.F., Kameyama, M., Kuhl, D.E., 1982. Evaluation of [^{123}I]isopropylidoamphetamine as a tracer for local cerebral blood flow using direct autoradiographic comparison. *J. Cereb. Blood Flow Metab.* 2, 179–185.
- Meikle, S.R., Hutton, B.F., Bailey, D.L., 1994. A transmission-dependent method for scatter correction in SPECT. *J. Nucl. Med.* 35, 360–367.
- Mintun, M.A., Raichle, M.E., Martin, W.R., Herscovitch, P., 1984. Brain oxygen utilization measured with O-15 radiotracers and positron emission tomography. *J. Nucl. Med.* 25, 177–187.
- Narita, Y., Eberl, S., Iida, H., Hutton, B.F., Braun, M., Nakamura, T., Bautovich, G., 1996. Monte Carlo and experimental evaluation of accuracy and noise properties of two scatter correction methods for SPECT. *Phys. Med. Biol.* 41, 2481–2496.
- Nishizawa, S., Iida, H., Tsuchida, T., Ito, H., Konishi, J., Yonekura, Y., 2003. Validation of the Dual-Table autoradiographic method to quantify two sequential rCBFs in a single SPET session with *N*-isopropyl- ^{123}I *p*-iodoamphetamine. *Eur. J. Nucl. Med. Mol. Imaging* 30, 943–950.
- Oku, N., Matsumoto, M., Hashikawa, K., Moriwaki, H., Okazaki, Y., Seike, Y., Handa, N., Uehara, T., Kamada, T., Nishimura, T., 1994. Carbon dioxide reactivity by consecutive technetium-99m-HMPAO SPECT in patients with a chronically obstructed major cerebral artery. *J. Nucl. Med.* 35 (1), 32–40.
- Powers, W.J., 1991. Cerebral hemodynamics in ischemic cerebrovascular disease. *Ann. Neurol.* 29, 231–240.
- Powers, W.J., Raichle, M.E., 1985. Positron emission tomography and its application to the study of cerebrovascular disease in man. *Stroke* 16, 361–376.
- Silbersweig, D.A., Stern, E., Frith, C.D., Cahill, C., Schnorr, L., Grootenok, S., Spinks, T., Clark, J., Frackowiak, R., Jones, T., 1993. Detection of thirty-second cognitive activations in single subjects with positron emission tomography: a new low-dose $H_2^{18}O$ regional cerebral blood flow three-dimensional imaging technique. *J. Cereb. Blood Flow Metab.* 13, 617–629.
- Silbersweig, D.A., Stern, E., Schnorr, L., Frith, C.D., Ashburner, J., Cahill, C., Frackowiak, R.S., Jones, T., 1994. Imaging transient, randomly occurring neuropsychological events in single subjects with positron emission tomography: an event-related count rate correlational analysis. *J. Cereb. Blood Flow Metab.* 14, 771–782.
- The-EC/IC-Bypass-Study-Group, 1985a. Failure of extracranial intracranial arterial bypass to reduce the risk of ischemic stroke. Results of an international randomized trial. *N. Engl. J. Med.* 313, 1191–1200.
- The-EC/IC-Bypass-Study-Group, 1985b. The international cooperative study of extracranial/intracranial arterial anastomosis (EC/IC bypass study): methodology and entry characteristics. *Stroke* 16, 397–406.
- Vortrup, S., Henriksen, L., Paulson, O.B., 1984. Effect of acetazolamide on cerebral blood flow and cerebral metabolic rate of oxygen. *J. Clin. Invest.* 74, 1634–1639.
- Vortrup, S., Brun, B., Lassen, N.A., 1986. Evaluation of the cerebral vasodilatory capacity by the acetazolamide test before EC-IC bypass surgery in patients with occlusion of the internal carotid artery. *Stroke* 17, 1291–1298.
- Watabe, H., Kondoh, Y., Kim, K.M., Shidahara, M., Iida, H. (Eds.), 2002. Shortening rCBF Measurement Interval in [^{18}O]H₂O PET. Brain Imaging Using PET. Academic Press, San Diego.
- Yamaguchi, T., Kanno, I., Uemura, K., Shishido, F., Inugami, A., Ogawa, T., Murakami, M., Suzuki, K., 1986. Reduction in regional cerebral metabolic rate of oxygen during human aging. *Stroke* 17, 1220–1228.

The association between the Val158Met polymorphism of the catechol-O-methyl transferase gene and morphological abnormalities of the brain in chronic schizophrenia

Takashi Ohnishi,^{1,2,4} Ryota Hashimoto,² Takeyuki Mori,^{1,2} Kiyotaka Nemoto,¹ Yoshiya Moriguchi,¹ Hidehiro Iida,⁴ Hiroko Noguchi,² Tetsuo Nakabayashi,^{2,3} Hiroaki Hori,^{2,3} Mayu Ohmori,³ Ryoutaro Tsukue,³ Kimitaka Anami,³ Naotugu Hirabayashi,³ Seiichi Harada,³ Kunimasa Arima,³ Osamu Saitoh³ and Hiroshi Kunugi²

¹Department of Radiology, National Center Hospital of Mental, Nervous and Muscular Disorders, National Center of Neurology and Psychiatry, ²Department of Mental Disorder Research, National Institute of Neuroscience, National Center of Neurology and Psychiatry, ³Department of Psychiatry, National Center Hospital of Mental, Nervous, and Muscular Disorders, National Center of Neurology and Psychiatry, Tokyo and ⁴Department of Investigative Radiology, Research Institute, National Cardiovascular Center, Osaka, Japan

Correspondence to: Takashi Ohnishi, Department of Radiology, National Center Hospital of Mental, Nervous, and Muscular Disorders, National Center of Neurology and Psychiatry 4-1-1 Ogawa Higashi, Kodaira City, Tokyo, Japan 187-0031
E-mail: tohnishi@hotmail.com

The catechol-O-methyl transferase (COMT) gene is considered to be a promising schizophrenia susceptibility gene. A common functional polymorphism (Val158Met) in the COMT gene affects dopamine regulation in the prefrontal cortex (PFC). Recent studies suggest that this polymorphism contributes to poor prefrontal functions, particularly working memory, in both normal individuals and patients with schizophrenia. However, possible morphological changes underlying such functional impairments remain to be clarified. The aim of this study was to examine whether the Val158Met polymorphism of the COMT gene has an impact on brain morphology in normal individuals and patients with schizophrenia. The Val158Met COMT genotype was obtained for 76 healthy controls and 47 schizophrenics. The diagnostic effects, the effects of COMT genotype and the genotype-diagnosis interaction on brain morphology were evaluated by using a voxel-by-voxel statistical analysis for high-resolution MRI, a tensor-based morphometry. Patients with schizophrenia demonstrated a significant reduction of volumes in the limbic and paralimbic systems, neocortical areas and the subcortical regions. Individuals homozygous for the Val-COMT allele demonstrated significant reduction of volumes in the left anterior cingulate cortex (ACC) and the right middle temporal gyrus (MTG) compared to Met-COMT carriers. Significant genotype-diagnosis interaction effects on brain morphology were noted in the left ACC, the left parahippocampal gyrus and the left amygdala-uncus. No significant genotype effects or genotype-diagnosis interaction effects on morphology in the dorsolateral PFC (DLPFC) were found. In the control group, no significant genotype effects on brain morphology were found. Schizophrenics homozygous for the Val-COMT showed a significant reduction of volumes in the bilateral ACC, left amygdala-uncus, right MTG and left thalamus compared to Met-COMT schizophrenics. Our findings suggest that the Val158Met polymorphism of the COMT gene might contribute to morphological abnormalities in schizophrenia.

Keywords: schizophrenia; polymorphism; COMT; ACC; DLPFC

Abbreviations: ACC = anterior cingulate cortex; COMT = catechol-O-methyl transferase; DLPFC = dorsolateral prefrontal cortex; FDR = false discovery rate; IQ = intelligence quotient; JART = Japanese version of National Adult Reading Test; ROI = region of interest; SPM = statistical parametric mapping; TBM = tensor-based morphometry

Received July 15, 2005. Revised September 21, 2005. Accepted October 27, 2005. Advance Access publication December 5, 2005

Introduction

Schizophrenia is a severe neuropsychiatric disorder with deficits of multiple domains of cognitive functions, volition and emotion. Family and twin studies have provided cumulative evidence for a genetic basis of schizophrenia (Kendler, 1983; McGue *et al.*, 1983; Sullivan *et al.*, 2003); however, identification of the underlying susceptibility loci has been limited. Collective data have suggested that the aetiology of schizophrenia involves the interplay of complex polygenic influences and environmental risk factors operating on brain maturational processes (Harrison *et al.*, 2005).

In vivo neuroimaging studies have demonstrated that brain abnormalities should play an important role in the pathophysiology of schizophrenia. Structural MRI studies have demonstrated relatively consistent brain abnormalities in patients with schizophrenia, such as enlargement of the ventricular system and regional volume decrease in the temporal lobe structures (Gaser *et al.*, 2001; Okubo *et al.*, 2001; Shenton *et al.*, 2001; Davidson and Heinrichs, 2003). Studies with schizophrenics and their healthy siblings demonstrate that even healthy siblings share some of morphological abnormalities observed in schizophrenia (Steel *et al.*, 2002; Gogtay *et al.*, 2003). A recent morphological MR study revealed that a common polymorphism of the brain-derived neurotrophic factor, one of the well-known schizophrenia susceptibility genes, affected the anatomy of the hippocampus and prefrontal cortex (PFC) in healthy individuals (Pezawas *et al.*, 2004). Furthermore, some studies have suggested that environmental factors interact with genetic factors (Cannon *et al.*, 1993; Nelson *et al.*, 2004). For example, obstetric complications are well known non-genetic risk factors of schizophrenia. However, a previous study suggested that obstetric complications might induce brain morphological abnormalities in schizophrenics and their siblings, but not in comparison with subjects at low genetic risk for schizophrenia (Cannon *et al.*, 1993). These facts suggest that genetic factors should have considerable impact on brain morphology in patients with schizophrenia.

Catechol-O-methyl transferase (COMT) is a promising schizophrenia susceptibility gene because of its role in monoamine metabolism (Goldberg *et al.*, 2003; Stefanis *et al.*, 2004; Harrison *et al.*, 2005). A common single nucleotide polymorphism (SNP) of the COMT gene producing an amino acid substitution of methionine (met) to valine (val) at position 108/158 (Val158Met) affects dopamine regulation in the PFC (Palmatier *et al.*, 1999). This polymorphism impacts on the stability of the enzyme, such that the Val-COMT allele has significantly lower enzyme activity than the Met-COMT allele (Weinberger *et al.*, 2001; Chen *et al.*, 2004). Several

studies have revealed that the Val-COMT allele is associated with poorer performances, compared to the Met-COMT allele, in cognitive tasks of frontal function such as the Wisconsin Card Sorting Test (WCST) and N-back task (Egan *et al.*, 2001; Weinberger *et al.*, 2001; Goldberg *et al.*, 2003). The underlying mechanism of such behavioural differences may be related to lower prefrontal dopamine levels arising from higher dopamine catabolism mediated by the Val-COMT allele (Chen *et al.*, 2004; Tunbridge *et al.*, 2004).

The results of studies on the association between the Val158Met polymorphism and schizophrenia have, however, been controversial (Daniels *et al.*, 1996; Kunugi *et al.*, 1997; Ohmori *et al.*, 1998; Norton *et al.*, 2002; Galderisi *et al.*, 2005; Ho *et al.*, 2005). The result of a meta-analysis was even more inconclusive (Fan *et al.*, 2005). Such inconsistency was also found in associations between frontal functions and the Val158Met polymorphism (Egan *et al.*, 2001; Weinberger *et al.*, 2001; Goldberg *et al.*, 2003; Ho *et al.*, 2005). The possible morphological changes due to the COMT gene might be present and play a role in susceptibility to schizophrenia and in giving rise to impaired frontal functions. However, morphological changes underlying functional impairments remain to be clarified.

A recent advancement of methods for MR volumetry, such as voxel-based morphometry and deformation-based morphometry [or tensor-based morphometry (TBM)], allows us to explore and analyse brain structures of schizophrenics (Wright *et al.*, 1995; Gaser *et al.*, 2001). Using TBM techniques, we investigated the association between the Val158-Met polymorphism of the COMT gene and brain morphology in normal individuals and patients with schizophrenia. The aim of this study was to clarify whether there are significant genotype and/or genotype-disease interaction effects on brain morphology.

Methods

Subjects

Seventy-six healthy subjects and forty-seven patients with schizophrenia participated in the study. All the subjects were biologically unrelated Japanese. Written informed consent was obtained from all the subjects in accordance with ethical guidelines set by a local ethical committee. All normal subjects were screened using a questionnaire on medical history and excluded if they had neurological, psychiatric or medical conditions that could potentially affect the CNS, such as substance abuse or dependence, atypical headache, head trauma with loss of consciousness, asymptomatic or symptomatic cerebral infarctions detected by T₂-weighted MRI, hypertension, chronic lung

disease, kidney disease, chronic hepatic disease, cancer, or diabetes mellitus. The patients were diagnosed on the basis of DSM-IV criteria, information from medical records and a clinical interview. All patients were stable and/or partially remitted at the time of MR measurement and neuropsychological tests.

According to genotypes, each group (control and schizophrenia) was categorized into three groups; the homozygous Val-COMT group (control: $n = 38$, two were left-handed, schizophrenia: $n = 19$, one was left-handed), the Val/Met-COMT group (control: $n = 25$, three were left-handed, schizophrenia: $n = 22$, all were right-handed) and the remaining homozygous Met-COMT group (control: $n = 13$, all were right-handed, schizophrenia: $n = 6$, all were right-handed). Because of the small number of subjects with homozygous Met-COMT, the Val/Met-COMT and homozygous Met-COMT groups were combined and treated as one group, the Met-COMT carriers. Table 1 shows the characteristics of each group. All groups were of comparable age, gender (χ^2 test, $df = 3$, $P = 0.38$) and handedness (χ^2 -test, $df = 3$, $P = 0.53$). No genotype effects and genotype-diagnosis interaction effects were found in years of education, scores of full scale Intelligence Quotient (IQ) and scores of premorbid IQ [Japanese version of National Adult Reading Test (JART) score], however, patients who had fewer years of education ($P < 0.0001$), had lower scores of both full scale IQ and JART ($P < 0.001$). The duration of illness, medication and hospitalization, the age at disease onset and drug dose (chlorpromazine equivalent) of those homozygous for the Val-COMT did not differ from the Met-COMT carriers.

SNP genotyping

Venous blood was drawn from subjects and genomic DNA was extracted from whole blood according to the standard procedures. The Val158Met polymorphism of the COMT gene (dbSNP accession: rs4680) was genotyped using the TaqMan 5'-exonuclease allelic discrimination assay, described previously (Hashimoto *et al.*, 2004, 2005). Briefly, primers and probes for detection of the SNP are: forward primer 5'-GACTGTGCCGCCATCAC-3', reverse primer 5'-CAGGCATGCACCTTGTC-3', probe 1 5'-VIC-TTTCGCTG-GCGTGAAG-MGB-3' and probe 2 5'-FAM-CGCTGGCATGAAG-MGB-3'. PCR cycling conditions were: at 95°C for 10 min, 50 cycles of 92°C for 15 s and 60°C for 1 min.

MRI procedures

All MR studies were performed on a 1.5 tesla Siemens Magnetom Vision plus system. A three dimensional (3D) volumetric acquisition of a T₁-weighted gradient echo sequence produced a gapless series of thin sagittal sections using an MPRage sequence (TE/TR, 4.4/11.4 ms; flip angle, 15°; acquisition matrix, 256 × 256; 1 NEX, field of view, 31.5 cm; slice thickness, 1.23 mm).

Image analysis (TBM)

The basic principle of TBM is to analyse the local deformations of an image and to infer local differences in brain structure. In TBM, MRI scans of individual subjects are mapped to a template image with three-dimensional (3D) non-linear normalization routines. Local deformations were estimated by a univariate Jacobian approach. The basic principle of TBM is the same as a method used in a previous report described as deformation-based morphometry (Gaser *et al.*, 2001). Firstly, inhomogeneities in MR images were corrected using a bias correction function in statistical parametric mapping (SPM2),

then the corrected image was scalp-edited by masking with a probability image of brain tissue obtained from each image using a segmentation function in SPM2. Using a linear normalization algorithm in SPM2, all brains were resized to a voxel size of 1.5 mm and adjusted for orientation and overall width, length and height (Fig. 1A). Therefore, brains were transformed to the anatomical space of a template brain whose space is based on Talairach space (Talairach and Tournoux, 1988). Subsequent non-linear normalization introduced local deformations to each brain to match it to the same scalp-edited template brain (Fig. 1C). The non-linear transformation was done using the high-dimension-warping algorithm (Ashburner and Friston, 2004). After the high dimensional warping, each image (Fig. 1B) looks similar to the template (Fig. 1C). Figure 2 demonstrated a mean MR image of 76 controls (left) and a mean MR image of 47 schizophrenics after high dimensional warping (Fig. 2). We obtained 3D deformation fields for every brain (Fig. 1D). Each of these 3D deformation fields consists of displacement vectors for every voxel, which describe the 3D displacement needed to locally deform the brain to match it to the template. We calculated the Jacobian determinants to obtain voxel by voxel parametric maps of local volume change relative to the template brain (Fig. 1E). The local Jacobian determinant is a parameter commonly used in continuum mechanics (Gurtin, 1987), which characterizes volume changes, such as local shrinkage or enlargement caused by warping. The parametric maps of Jacobian determinants were analysed using SPM2, which implements a 'general linear model'. To test hypotheses about regional population effects and interaction, data were analysed by an analysis of covariance (ANCOVA) without global normalization. There was no significant difference in age among the four groups, however, patients with schizophrenia, particularly those homozygous for the Val-COMT allele, were older than controls. Therefore, we treated age and years of education and scores of JART as nuisance variables. Since TBM explores the entire brain (grey matter, CSF space and white matter) at once, the search volume of TBM has a large number of voxels and since our interest was in morphological changes in the grey matter and CSF space, we excluded white matter tissue from analyses by using an explicit mask (Fig. 1F). We used $P < 0.001$, corrected for multiple comparisons with false discovery rate (FDR) < 0.05 as a statistical threshold. The resulting sets of t values constituted the statistical parametric maps {SPM (t)}. Firstly, we estimated the main effects, the genotype effect in total subjects (the Val/Val-COMT versus the Met-COMT carriers) and the diagnostic effect (schizophrenia versus controls) and then the genotype-diagnosis interaction effect was estimated. Furthermore, the effects of genotypes in each group (controls carrying the Val/Val-COMT gene versus controls carrying the Met-COMT gene and schizophrenics carrying the Val/Val-COMT gene versus schizophrenics carrying the Met-COMT gene) were estimated within the ANCOVA design matrix. Anatomical localization accorded both to MNI coordinates and Talairach coordinates obtained from M. Brett's transformations (www.mrc-cbu.cam.ac.uk/Imaging/mninspace.html) and are presented as Talairach coordinates (Talairach and Tournoux, 1988). Since previous studies have demonstrated the association between the Val158Met polymorphism and the dorsolateral PFC (DLPFC), we applied an additional hypothesis-driven region of interest (ROI) method to test regional population effects in the DLPFC. For this ROI analysis, we used the Wake Forest University PickAtlas (Maldjian *et al.*, 2003) within the ANCOVA design matrix for SPM analysis. We set $P < 0.05$ (uncorrected) with a small volume correction ($P < 0.05$ within the ROI) to assess grey matter volume changes in the DLPFC (Brodmann area 46, 9 and 8).

Table 1 Subject characteristics

	Control Val/Val	Met carriers	Schizophrenia Val/Val	Met carriers	Diagnosis F (P)	Genotype F (P)*	Genotype by diagnosis F (P)
Number of subjects	38	38	19	28			
Gender (M/F)	16 out of 22	14 out of 24	11 out of 8	13 out of 15			
Handedness (R/L)	36 out of 2	35 out of 3	18 out of 1	28 out of 0			
Age (years)	41.47 (13.42)	39.26 (10.6)	45.98 (15.29)	43.05 (10.57)	3.633 (0.059)	1.7 (0.195)	0.21 (0.647)
Education (years)	17 (3.16)	16.06 (2.57)	12.67 (2.43)	13.33 (3.31)	30.855 (<0.0001)	0.047 (0.828)	1.61 (0.208)
Full scale IQ (WAIS-R)	113.42 (12.05)	108.93 (13.58)	80.69 (17.68)	88.958 (22.08)	57.9 (<0.001)	0.29 (0.59)	3.41 (0.068)
JART	78.8 (10.45)	75.42 (13.65)	54.69 (20.74)	62.25 (27.06)	23.366 (<0.001)	0.292 (0.59)	2.014 (0.159)
Wechsler Memory Scale—Revised							
Verbal memory	111.78 (15.001)	111.061 (12.89)	78.0 (21.623)	81.33 (18.57)	86.93 (<0.001)	0.147 (0.702)	0.354 (0.553)
Visual memory	112.1 (8.51)	106.55 (11.99)	74.78 (24.32)	83.29 (20.613)	85.51 (<0.001)	0.204 (0.65)	4.605 (0.03)
General memory	113.31 (13.92)	110.85 (12.22)	74.43 (21.3)	79.33 (19.14)	111.93 (<0.001)	0.135 (0.715)	1.226 (0.27)
Attention/concentration	104.47 (13.25)	102.94 (16.51)	87.79 (19.09)	92.54 (17.38)	16.08 (0.001)	0.228 (0.634)	0.866 (0.14)
Delayed recall	111.88 (15.46)	112.48 (10.08)	77.07 (20.92)	81.21 (19.19)	99.74 (<0.001)	0.52 (0.475)	0.284 (0.59)
WCST (preservative error)	2.5 (3.89)	3.14 (3.90)	12.08 (11.54)	8.52 (10.63)	24.5 (<0.0001)	0.93 (0.34)	1.93 (0.17)
Digit span	11.12 (3.25)	10.77 (3.34)	7.83 (3.93)	9.09 (2.74)	12.165 (0.0007)	0.415 (0.52)	1.28 (0.261)
Onset age			25.38 (10.34)	23.74 (7.992)		0.52	
Duration of illness (years)			19.86 (14.93)	18.84 (9.8)		0.77	
Duration of hospitalization (months)			66 (153.41)	59.59 (91.18)		0.86	
Duration of medication (years)			12.86 (14.21)	16.4 (9.89)		0.29	
Drug dose of typical antipsychotic drugs (mg/dsy; chlorpromazine equivalent)			617.9 (720.18)	700.38 (752.67)		0.69	
Drug dose of atypical antipsychotic drugs (mg/dsy; chlorpromazine equivalent)							
Mean (standard deviation)			282.3 (428.29)	340.23 (482.19)		0.66	

Mean (standard deviation); WAIS-R = Wechsler Adult Intelligence Scale—Revised; JART = Japanese version of National Adult Reading Test; WCST = Wisconsin Card Sorting Test.

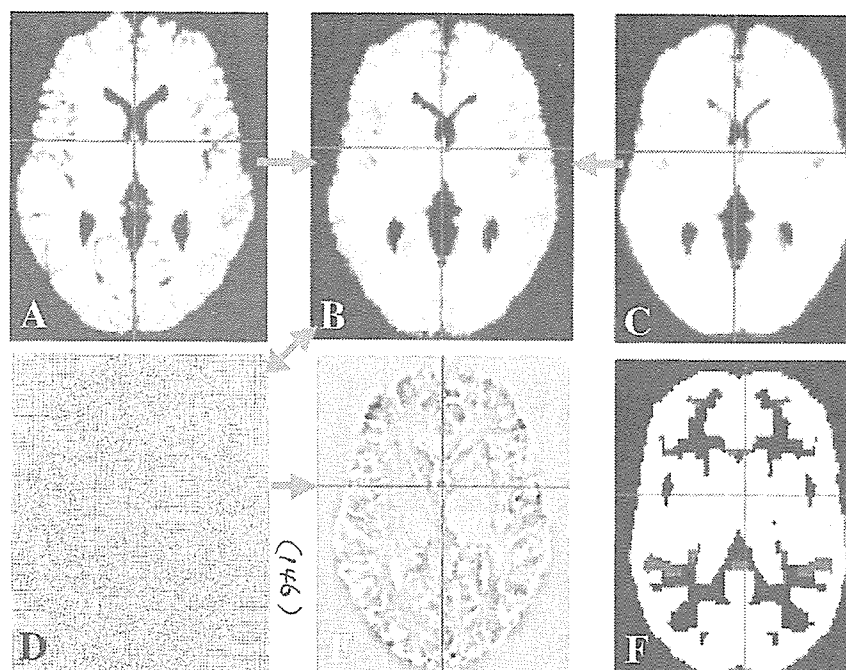


Fig. 1 Steps of analysis for tensor-based morphometry. An example is shown for a single subject in one axial slice. The single object brain (A) has been corrected for orientation and overall size to the template brain (C). Non-linear spatial normalization removes most of the anatomical differences between the two brains by introducing local deformations to the object brain, which then (B) looks as similar as possible to the template. Image (D) shows the deformations applied to the object brain by a deformed grid. Statistical analysis can be done univariate using the local Jacobian determinant as a derivative of the field (E). An explicit mask image (F) was used to explore morphology in the grey matter and CSF space.

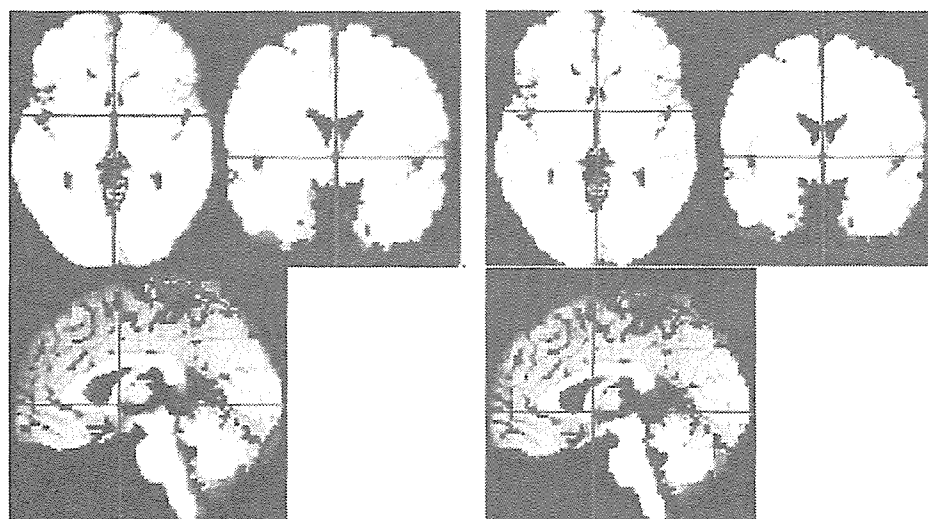


Fig. 2 Mean images after high dimensional warping control subjects and schizophrenics. *Left:* The mean image of warped MR images obtained from 76 controls. Even after averaging, the mean image is not blurred. *Right:* The mean image of warped MR images obtained from 47 schizophrenics. The mean image of schizophrenic looks similar to that of controls.

Results

Behavioural data

Patients had a lower full scale IQ, measured by the Wechsler Adult Intelligence Scale—Revised, than controls. They also had a lower expected premorbid IQ measured by a IART,

lower scores of Wechsler Memory Scale—Revised and demonstrated poorer performance of working memory measures such as the number of preservative errors in the WCST and digit span (Table 1). No genotype or genotype-diagnosis interaction effects were found in working memory measures

Table 2 Results of image analyses

Anatomical regions	Brodmann area	Cluster size	Corrected P FDR	T-value (voxel level)	Talairach coordinates		
					x	y	z
Main effects							
Diagnosis effects (control > schizophrenia) (Fig. 3)							
Limbic system							
R insula	BA13	4682	0.000	6.41	33	11	-2
L insula	BA13	4017	0.000	8.81	33	11	4
R parahippocampal gyrus, amygdala-uncus	BA36	4682	0.000	7.32	30	1	-17
R parahippocampal gyrus	BA36	186	0.000	5.04	30	-41	-8
L parahippocampal gyrus, hippocampus-amygdala	BA34/36	637	0.000	5.46	-20	-41	-8
R anterior cingulate cortex	BA32	147	0.000	4.9	9	33	20
L anterior cingulate cortex	BA32	200	0.000	4.63	11	32	20
L cingulate gyrus	BA32	275	0.001	4.2	-12	-16	39
Prefrontal cortex							
R inferior frontal gyrus	BA47,11	145	0.000	4.99	27	28	-11
R superior frontal gyrus	BA8/9	1889	0.000	6.08	12	43	39
L medial frontal gyrus	BA9	1333	0.000	5.13	-8	47	19
L inferior frontal gyrus	BA45	141	0.000	4.55	-44	23	15
L middle frontal gyrus	BA8	482	0.000	4.44	-30	24	43
L superior frontal gyrus	BA8	482	0.000	4.39	-35	17	51
Premotor area							
R dorsal premotor area	BA6	429	0.000	4.37	41	13	45
Temporal cortex							
R superior temporal gyrus	BA22	806	0.000	5.04	47	23	1
R middle temporal gyrus	BA21	806	0.000	4.87	56	-15	-3
L superior temporal gyrus	BA38	4017	0.000	7	-36	1	-17
Central grey matter							
L thalamus		4017	0.000	7.26	-15	-17	2
Diagnosis effects (control < schizophrenia) (Fig. 4)							
L sylvian fissure		621	0.000	6.7	45	17	3
R sylvian fissure		774	0.000	6.59	44	17	-8
Lateral ventricle (anterior horn)		279	0.000	5.27	-5	21	4
Lateral ventricle (L inferior horn)		248	0.000	6.18	-41	-30	-10
Lateral ventricle (R inferior horn)		137	0.000	5.02	36	-40	-1
Interhemispheric fissure		154	0.000	5.28	3	55	12
Genotype effects (Val/Val-COMT < Met-COMT carriers) (Fig. 5)							
Limbic system							
L anterior cingulate cortex	BA24/25	334	0.033	4.29	-8	17	-13
Temporal cortex							
R middle temporal gyrus	BA21	285	0.016	5.10	59	-3	14
Genotype-diagnosis interaction effects (Fig. 6)							
Limbic system							
L anterior cingulate gyrus	BA24/25/32	264	0.044	3.77	-6	25	-6
L parahippocampal gyrus, amygdala-uncus	BA34	219	0.048	3.74	-24	-6	-14
The effects of polymorphism in control group (no significant difference)							
The effects of polymorphism in schizophrenia							
Val/Val-COMT < Val/Met, Met/Met-COMT (Fig. 7)							
Limbic system							
L parahippocampal gyrus, amygdala-uncus	BA28	81	0.010	4.17	-26	2	22
L anterior cingulate cortex	BA24/25/32	263	0.007	4.38	-7	20	-8
Central grey matter							
L thalamus		91	0.014	3.94	-21	-28	6

and IQ, however, a significant genotype-by-diagnosis interaction effect was found in a visual memory measure ($F = 4.605$, $df = 1$, $P = 0.03$) (Table 1). However, a *post hoc t*-test (Bonferroni test) demonstrated no genotype effect in each diagnostic category (control: $P = 0.15$, schizophrenia: $P = 0.11$).

Morphological changes in schizophrenia (diagnosis effects)

In comparison with controls, patients with schizophrenia demonstrated a significant reduction of volumes in multiple brain areas, such as the limbic and paralimbic systems, neocortical areas and the subcortical regions (Table 2 and Fig. 3).

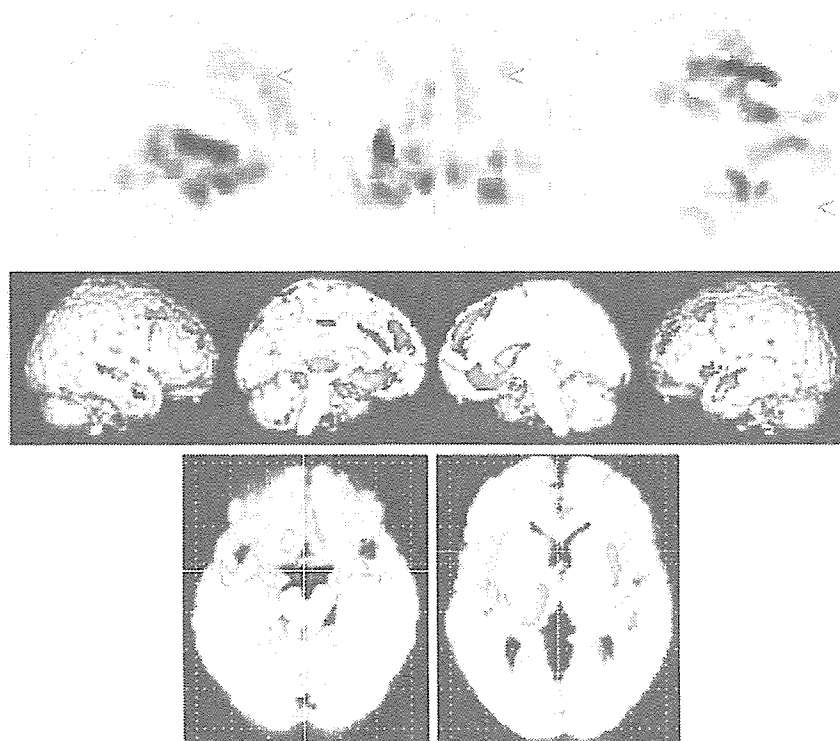


Fig. 3 Decreased volumes in schizophrenics ($n = 47$) as compared to controls ($n = 76$). *Top*: The SPM $\{t\}$ is displayed in a standard format as a maximum-intensity projection (MIP) viewed from the right, the back and the top of the brain. The anatomical space corresponds to the atlas of Talairach and Tournoux. Representation in stereotaxic space of regions with significant reduction of volume in schizophrenia was demonstrated. Schizophrenics demonstrated a significant reduction of volumes in the multiple brain areas, such as the limbic and paralimbic systems, neocortical areas and the subcortical regions. *Middle*: The SPM $\{t\}$ is rendered onto T_1 -weighted MR images. *Bottom*: The SPM $\{t\}$ is displayed onto axial T_1 -weighted MR images. A significantly decreased volume of the amygdala-uncus, bilateral insular cortices, ACC, temporal cortex and the left thalamus in schizophrenics was noted.

In the limbic and paralimbic systems, patients with schizophrenia showed reduction of volumes in the parahippocampal gyri, amygdala-uncus, insular cortices and the anterior cingulate cortices (ACC). They also demonstrated reduced volumes in the frontal and temporal association areas, dorsal premotor areas and the left thalamus. In comparison with controls, patients with schizophrenia showed significantly increased volume in the CSF space such as lateral ventricle, sylvian and the interhemispheric fissures but not in the grey matter (Table 2 and Fig. 4).

Morphological changes associated with the Val158Met polymorphism (genotype effects)

In comparison with Met-COMT carriers, individuals homozygous for the Val-COMT allele demonstrated a significant reduction of volumes in the left ACC and the right middle temporal gyrus (MTG) (Table 2 and Fig. 5). The hypothesis-driven analysis demonstrated a genotype effect on volumes in the bilateral DLPFC (right BA9, left BA8) at a lenient threshold (uncorrected $P = 0.05$) (data are not shown), however, no voxels could survive after the correction for multiple

comparisons ($FDR < 0.05$) within the ROI. There were no areas that individuals homozygous for the Val-COMT allele demonstrated a significant increment of volume compared to Met-COMT carriers.

Genotype–diagnosis interaction effects

We found significant genotype-diagnosis interaction effects on brain morphology. The stronger effects of Val158Met polymorphism on brain morphology in schizophrenia than those in controls were noted in the left ACC and the left amygdala-uncus (Table 2 and Fig. 6). The hypothesis-driven analysis demonstrated a genotype-diagnosis interaction effect on the volume of the right DLPFC (BA9/46) at a lenient threshold (uncorrected $P = 0.05$) (data not shown), however, no voxels could survive after the correction of multiple comparisons ($FDR < 0.05$) within the ROI.

Effects of the Val158Met polymorphism on brain morphology

Since genotype–disease interaction effects were found, we estimated the effects of genotypes on brain morphology in the control groups and the schizophrenic groups separately.

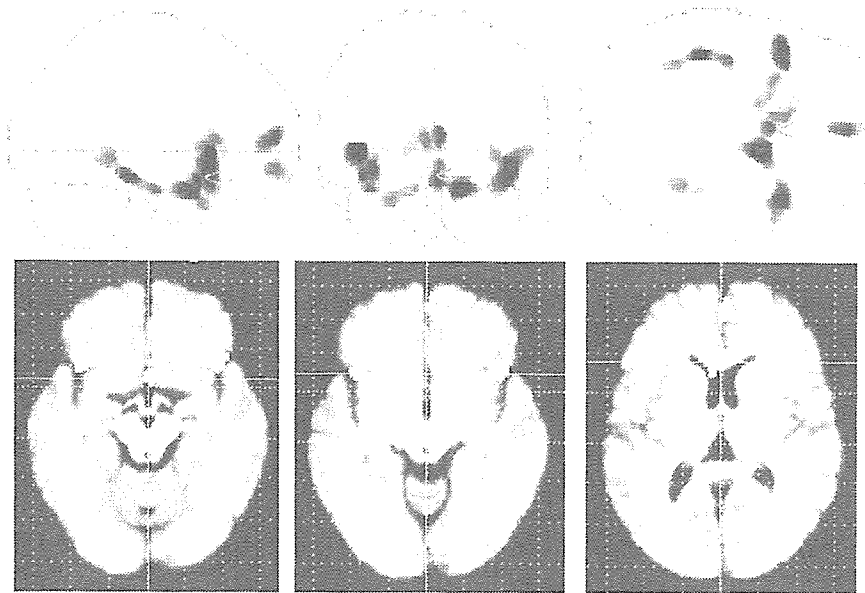


Fig. 4 Increased volumes in schizophrenics as compared to controls. *Top*: The SPM $\{t\}$ is displayed in a standard format as a MIP. Patients with schizophrenia showed a significantly increased volume of the CSF space. *Bottom*: The SPM $\{t\}$ is displayed onto axial T_1 -weighted MR images. A significantly increased volume of the CSF space such as the lateral ventricle, sylvian fissures and the interhemispheric fissure was noted.

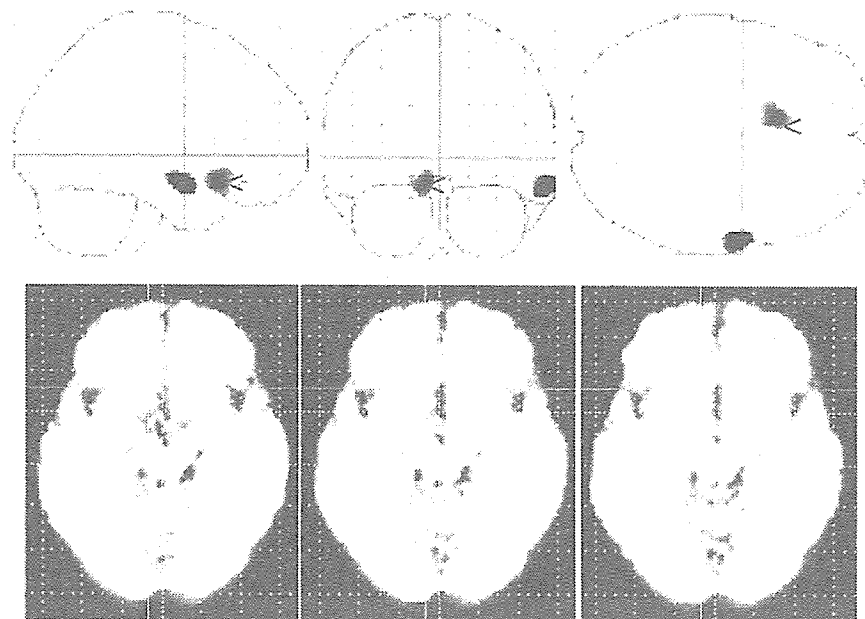


Fig. 5 The result of comparison between individuals homozygous for the Val-COMT allele ($n = 57$) and Met-COMT carriers ($n = 66$) (genotype effects). *Top*: Representation in stereotaxic space of regions with significant reduction of volume in individuals homozygous for the Val-COMT allele demonstrated. *Bottom*: The SPM $\{t\}$ is displayed onto axial T_1 -weighted MR images. Individuals homozygous for the Val-COMT allele demonstrated a significant reduction of volumes in the left ACC and right MTG as compared to Met-COMT carriers.

In the control group, we found no significant morphological differences between individuals homozygous for the Val-COMT allele and Met-COMT carriers. Even the hypothesis driven analysis with a lenient statistical threshold ($P < 0.05$) could not detect any significant morphological changes in the

DLPFC between the two groups. Contrary to the control group, schizophrenics homozygous for the Val-COMT allele showed a significant reduction of volumes in the left amygdala-uncus, bilateral ACC, right MTG and the left thalamus when compared to the patients carrying the Met-COMT

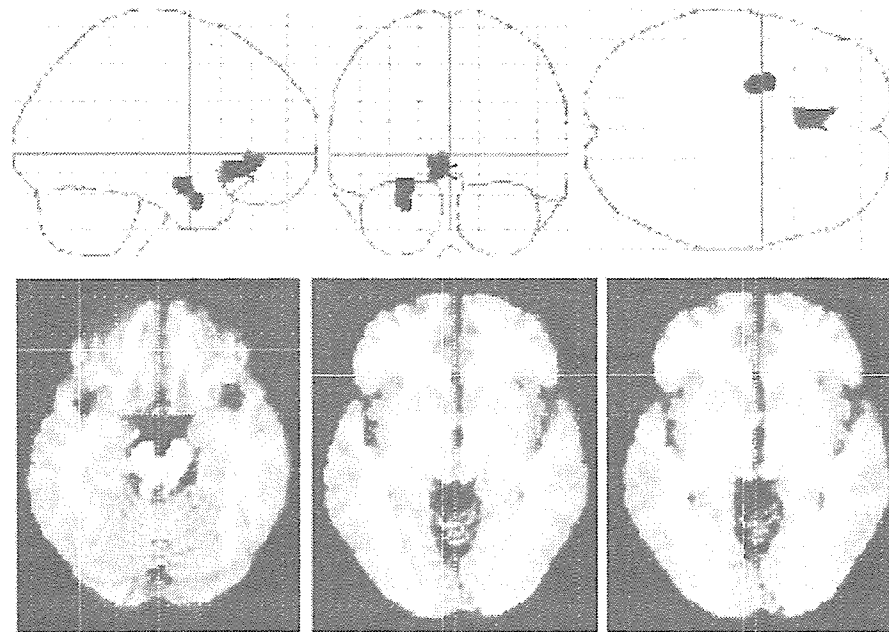


Fig. 6 Results of genotype-diagnosis interaction effects on brain morphology. *Top:* The SPM $\{t\}$ is displayed in a standard format as a MIP. The stronger effects of Val158Met polymorphism on brain morphology in schizophrenia than those in controls were noted in the left ACC, left parahippocampal gyrus and the amygdala-uncus. *Bottom:* The SPM $\{t\}$ is displayed onto axial T_1 -weighted MR images.

allele (Table 2, Fig. 7). The hypothesis-driven analysis demonstrated a significantly decreased volume of the bilateral DLPFC in schizophrenics homozygous for the Val-COMT allele when compared to the Met-COMT schizophrenics at a lenient threshold (uncorrected $P = 0.05$) (data not shown). However, no voxels could survive after the correction for multiple comparisons ($FDR < 0.05$) within the ROI. There are no significantly increased volumes in the schizophrenics homozygous for the Val-COMT allele. All the results were essentially unchanged even if all the left-handed subjects were excluded in all analyses (data not shown).

Discussion

In this study, we found reduction of volumes in the limbic and paralimbic systems, neocortical areas (prefrontal and temporal cortices) and thalamus in patients with schizophrenia when compared to control subjects. The schizophrenia patients demonstrated a significant enlargement of CSF spaces including the lateral and sylvian fissure, which could be interpreted as a result of impaired neurodevelopment and/or global brain atrophy. These findings are concordant with previous studies of MR morphometry of schizophrenia. According to a recent review and meta-analyses of the morphometry of schizophrenia, the consistent abnormalities in schizophrenia are as follows; (i) ventricular enlargement (lateral and third ventricles); (ii) medial temporal lobe involvement; (iii) superior temporal gyrus involvement (iv) parietal lobe involvement; and (v) subcortical brain region

involvement including the thalamus (Okubo *et al.*, 2001; Shenton *et al.*, 2001; Davidson and Heinrichs, 2003). The other regions observed in this study, such as the insula, DLPFC and the ACC have also often been demonstrated as abnormal areas in schizophrenia (Shenton *et al.*, 2001; Takahashi *et al.*, 2004; Yamasue *et al.*, 2004). Using the TBM technique, we replicated the morphological abnormalities observed in previous MR studies on schizophrenia, suggesting that TBM was able to detect morphological changes associated with this disease. As well as neuroimaging studies, post-mortem studies have also reported morphological abnormalities in schizophrenia, but not necessarily as common neuropathological features. Regions including the hippocampus, ACC, thalamus and the DLPFC are regularly associated with abnormalities of cell size, cell number and neuronal organization (Bogerts, 1993; Arnold and Trojanowski, 1996; Selemon, 2001; Selemon and Lynn, 2002, 2003). Selemon *et al.* reported that schizophrenics demonstrated abnormalities in overall and laminar neuronal density in the DLPFC (Brodmann area 9) and suggested that the DLPFC should be a particularly vulnerable target in the disease process (Selemon 2001; Selemon and Lynn, 2002, 2003).

Importantly, our results suggest that some of the morphological changes in schizophrenia mentioned above are associated with the Val158Met polymorphism of the COMT gene. In the schizophrenic group, the polymorphism was associated with the volumes in the limbic and paralimbic systems, temporal cortices and the left thalamus, whereas no morphological changes related to the polymorphism were found in

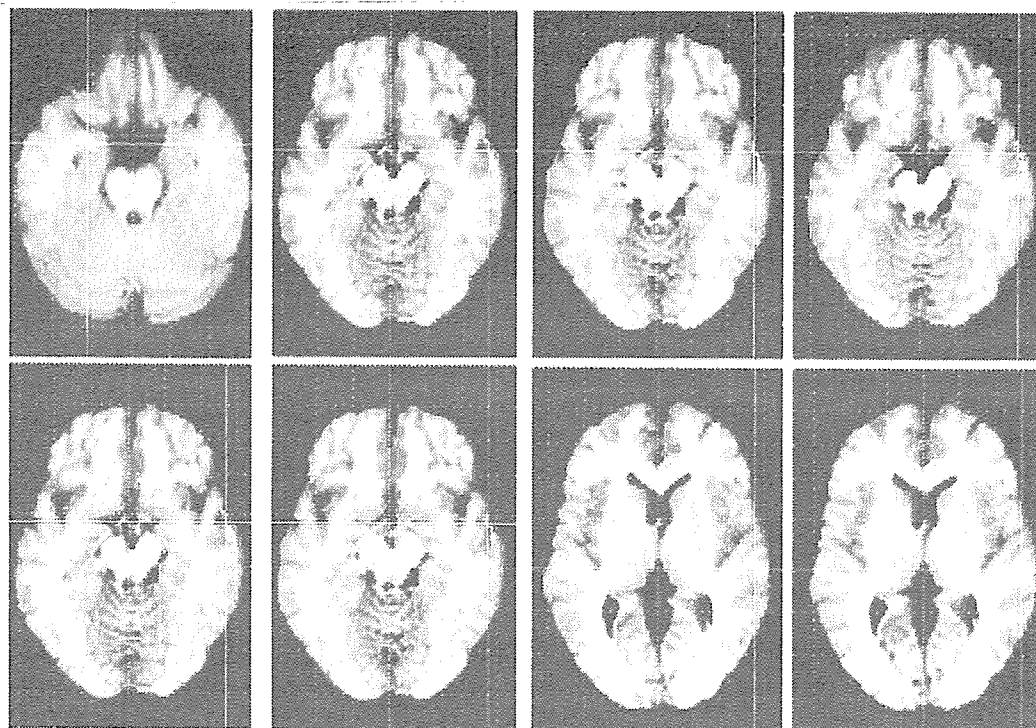


Fig. 7 The effects of the Val158Met polymorphism of the COMT gene on brain morphology in schizophrenics. The SPM (t) is displayed onto axial T_1 -weighted MR images. The schizophrenics homozygous for the Val-COMT allele ($n = 19$) showed a significant reduction of volumes in the left parahippocampal gyrus, amygdala-uncus, ACC, left thalamus and the right MTG when compared to patients who carried the Met-COMT allele ($n = 28$).

normal individuals. As a consequence, significant genotype-diagnosis interaction effects were found in the left ACC and the amygdala-uncus. These results indicate that the Val158-Met polymorphism of the COMT gene is strongly associated with morphological changes in schizophrenia, particularly those in the limbic and paralimbic systems. Longitudinal MRI studies of schizophrenia strongly suggest that progressive changes should occur after onset of the illness (Okubo *et al.*, 2001; Ho *et al.*, 2003). Recent studies have demonstrated that antipsychotic drugs, particularly haloperidol, have considerable effects on brain morphology (Arango *et al.*, 2003; Lieberman, 2005; Dorph *et al.*, 2005). Because of the long duration of illness and medication taken by our subjects, the effects of antipsychotics may be a possible confounding factor for our findings. However, the duration of medication and the dose of antipsychotics taken by the Val/Val-COMT schizophrenics did not differ from those of the Met-COMT schizophrenics. Although the effects of antipsychotics on brain morphology may contribute to the observed morphological changes in patients with schizophrenia in this study, it is unlikely that the effects of antipsychotics contributed to morphological differences between the two schizophrenic groups.

When we were preparing this manuscript, another study demonstrated no genotype and genotype-diagnosis interaction effects of the Val158Met polymorphism on morphology of the frontal lobe in controls and schizophrenia (Ho *et al.*,

2005). Although there are differences between the two studies, such as mean ages of subjects, duration of illness, methods for image analysis and a racial factor (Caucasians versus Japanese), that study also demonstrated no genotype and genotype-diagnosis interaction effects on morphology of the DLPFC. However, we found these effects on DLPFC morphology at a very lenient statistical threshold. Further studies with a larger sample will clarify whether Val158Met polymorphism does affect DLPFC morphology. As well as prefrontal morphology, we found no significant genotype or genotype-diagnosis interaction effects on working memory, however, schizophrenics homozygous for the Val-COMT allele tended to have poorer performances on working memory measures, compared to Met-COMT carriers with schizophrenia. Although there were no significant effects of Val158Met polymorphism on working memory and other neuropsychological measures, a significant effect of the polymorphism was noted in brain morphology. The brain morphology has been considered to be useful as an intermediate phenotype in genetic research in neuropsychiatric disorders (Baare *et al.*, 2001; Durston *et al.*, 2005). Therefore, morphological changes might be more sensitive to the effects of genotype than behavioural measures such as the performance of working memory measures. In a previous study (Ho *et al.*, 2005) a similar phenomenon—no significant effect of Val158Met polymorphism on working memory performance but significant

effects on brain activities during a working memory task—was found. Further studies with a larger sample size are needed to clarify whether morphological changes are a more sensitive marker of genotype effects than behavioural measures.

Unexpectedly, we found effects of the polymorphism on the ACC volume rather than the DLPFC which is crucial for working memory. Since the ACC is associated with a variety of cognitive tasks involving mental efforts, and also plays important roles in working memory (Paus *et al.*, 2001; Kondo *et al.*, 2004), it is feasible that the Val158Met polymorphism may be associated with the ACC morphology. In fact, a previous study demonstrated that the Val-COMT allele was associated with abnormal ACC function as well as abnormal prefrontal cortical function, relative to the Met-COMT allele, as measured by cognitive tests and fMRI activation in normal subjects (Egan *et al.*, 2001).

One would argue that the effects of one polymorphism of the gene could not explain the morphological changes in schizophrenia. As well as the effects of the Val158Met polymorphism, we agree that other polymorphisms of schizophrenia susceptibility genes and genotype–genotype interaction may relate to individual brain morphology. Such interactions might contribute to the different effects of the Val158Met polymorphism on brain morphology observed in this study. Further studies of each effect and interaction of several schizophrenia susceptibility genes on brain morphology, brain functions and performances of neuropsychological tests should be conducted to clarify how polymorphisms of these genes affect intermediate phenotypes of schizophrenia.

In conclusion, we found an association between the Val158Met polymorphism and morphological abnormalities in schizophrenia. Although the underlying mechanisms of our observation remain to be clarified, our data indicate that brain morphology as an intermediate phenotype should be useful for investigating how genotypes affect endophenotypes of schizophrenia.

Acknowledgements

This study was supported by the Promotion of Fundamental Studies in Health Science of Organization for Pharmaceuticals and Medical Devices Agency. This work was also supported in part by Grants-in-Aid from the Japanese Ministry of Health, Labor and Welfare (H17-kokoro-007 and H16-kokoro-002), the Japanese Ministry of Education, Culture, Sports, Science and Technology and Core research for Evolutional Science and Technology of Japan Science and Technology Agency, Japan Foundation for Neuroscience and Mental Health.

References

Arango C, Breier A, McMahon R, Carpenter WI Jr, Buchanan RW. The relationship of clozapine and haloperidol treatment response to prefrontal, hippocampal, and caudate brain volumes. *Am J Psychiatry* 2003; 160: 1421–7.

- Arnold SE, Trojanowski JQ. Recent advances in defining the neuropathology of schizophrenia. *Acta Neuropathol (Berl)* 1996; 92: 217–31.
- Ashburner J, Friston KJ. High-dimensional image warping. In: Frackowiak R, editor. *Human brain function*. 2nd edn. Academic Press; 2004. p. 673–94.
- Baare WF, Hulshoff Pol HE, Boomsma DI, Posthuma D, de Geus EJ, Schnack HG, et al. Quantitative genetic modeling of variation in human brain morphology. *Cereb Cortex* 2001; 11: 816–24.
- Bogerts B. Recent advances in the neuropathology of schizophrenia. *Schizophr Bull* 1993; 19: 431–45.
- Cannon TD, Mednick SA, Parnas J, Schulsinger F, Praestholm J, Vestergaard A. Developmental brain abnormalities in the offspring of schizophrenic mothers. I. Contributions of genetic and perinatal factors. *Arch Gen Psychiatry* 1993; 50: 551–64.
- Chen I, Lipska BK, Halim N, Ma QD, Matsumoto M, Melhem S, et al. Functional analysis of genetic variation in catechol-O-methyltransferase (COMT): effects on mRNA, protein, and enzyme activity in postmortem human brain. *Am J Hum Genet* 2004; 75: 807–21.
- Daniels JK, Williams NM, Williams J, Jones LA, Cardno AG, Murphy KC, et al. No evidence for allelic association between schizophrenia and a polymorphism determining high or low catechol O-methyltransferase activity. *Am J Psychiatry* 1996; 153: 268–70.
- Davidson LL, Heinrichs RW. Quantification of frontal and temporal lobe brain-imaging findings in schizophrenia: a meta-analysis. *Psychiatry Res* 2003; 122: 69–87.
- Dorph Petersen KA, Pierri JN, Perel JM, Sun Z, Sampson AR, Lewis DA. The influence of chronic exposure to antipsychotic medications on brain size before and after tissue fixation: a comparison of haloperidol and olanzapine in macaque monkeys. *Neuropsychopharmacology* 2005; 30: 1649–61.
- Durston S, Fossella JA, Casey BJ, Hulshoff Pol HE, Galvan A, Schnack HG, et al. Differential effects of DRD4 and DAT1 genotype on fronto-striatal gray matter volumes in a sample of subjects with attention deficit hyperactivity disorder, their unaffected siblings, and controls. *Mol Psychiatry* 2005; 10: 678–85.
- Egan MF, Goldberg TE, Kolachana BS, Callicott JH, Mazzanti CM, Straub RE, et al. Effect of COMT Val108/158 Met genotype on frontal lobe function and risk for schizophrenia. *Proc Natl Acad Sci USA* 2001; 98: 6917–22.
- Fan JB, Zhang CS, Gu NF, Li XW, Sun WW, Wang HY, et al. Catechol-O-methyltransferase gene Val/Met functional polymorphism and risk of schizophrenia: a large-scale association study plus meta-analysis. *Biol Psychiatry* 2005; 57: 139–44.
- Galerisi S, Maj M, Kirkpatrick B, Piccardi P, Mucci A, Invernizzi G, et al. COMT Val(158)Met and BDNF C(270)T polymorphisms in schizophrenia: a case-control study. *Schizophr Res* 2005; 73: 27–30.
- Gaser C, Nenadic I, Buchsbaum BR, Hazlett EA, Buchsbaum MS. Deformation-based morphometry and its relation to conventional volumetry of brain lateral ventricles in MRI. *Neuroimage* 2001; 13: 1140–5.
- Gogtay N, Sporn A, Clasen LS, Greenstein D, Giedd JN, Lenane M, et al. Structural brain MRI abnormalities in healthy siblings of patients with childhood-onset schizophrenia. *Am J Psychiatry* 2003; 160: 569–571.
- Goldberg TE, Egan MF, Gscheidle T, Coppola R, Weickert T, Kolachana BS, et al. Executive subprocesses in working memory: relationship to catechol-O-methyltransferase Val158Met genotype and schizophrenia. *Arch Gen Psychiatry* 2003; 60: 889–96.
- Gurtin, ME. *An introduction to continuum mechanics*. Boston: Academic Press; 1987.
- Harrison PJ, Weinberger DR. Schizophrenia genes, gene expression, and neuropathology: on the matter of their convergence. *Mol Psychiatry* 2005; 10: 40–68.
- Hashimoto R, Yoshida M, Ozaki N, Yamanouchi Y, Iwata N, Suzuki T, et al. Association analysis of the -308G>A promoter polymorphism of the tumor necrosis factor alpha (TNF-alpha) gene in Japanese patients with schizophrenia. *J Neural Transm* 2004; 111: 217–21.
- Hashimoto R, Yoshida M, Kunugi H, Ozaki N, Yamanouchi Y, Iwata N, et al. A missense polymorphism (H204R) of a Rho GTPase activating protein, the chimerin 2 gene, is associated with schizophrenia in men. *Schizophr Res* 2005; 73: 383–5.

- Ho BC, Andreasen NC, Nopoulos P, Arndt S, Magnotta V, Flaum M. Progressive structural brain abnormalities and their relationship to clinical outcome: a longitudinal magnetic resonance imaging study early in schizophrenia. *Arch Gen Psychiatry* 2003; 60: 585–94.
- Ho BC, Wassink TH, O'leary DS, Sheffield VC, Andreasen NC. Catechol-O-methyl transferase Val(158)Met gene polymorphism in schizophrenia: working memory, frontal lobe MRI morphology and frontal cerebral blood flow. *Mol Psychiatry* 2005; 10: 287–98.
- Kendler KS. Overview: a current perspective on twin studies of schizophrenia. *Am J Psychiatry* 1983; 140: 1413–25.
- Kondo H, Osaka N, Osaka M. Cooperation of the anterior cingulate cortex and dorsolateral prefrontal cortex for attention shifting. *Neuroimage* 2004; 23: 670–9.
- Kunugi H, Vallada HP, Sham PC, Hoda F, Arranz MJ, Li T, *et al.* Catechol-O-methyltransferase polymorphisms and schizophrenia: a transmission disequilibrium study in multiply affected families. *Psychiatr Genet* 1997; 7: 97–101.
- Lieberman JA, Tollefson GD, Charles C, Zipursky R, Sharma T, Kahn RS, *et al.* Antipsychotic drug effects on brain morphology in first-episode psychosis. *Arch Gen Psychiatry* 2005; 62: 361–70.
- Maldjian JA, Laurienti PJ, Kraft RA, Burdette JH. An automated method for neuroanatomic and cytoarchitectonic atlas-based interrogation of fMRI data sets. *Neuroimage* 2003; 19: 1233–9.
- McGue M, Gottesman II, Rao DC. The transmission of schizophrenia under a multifactorial threshold model. *Am J Hum Genet* 1983; 35: 1161–78.
- Nelson KB, Lynch IK. Stroke in newborn infants. *Lancet Neurol* 2004; 3: 150–8.
- Norton N, Kirov G, Zammit S, Jones G, Jones S, Owen R, *et al.* Schizophrenia and functional polymorphisms in the MAOA and COMT genes: no evidence for association or epistasis. *Am J Med Genet* 2002; 114: 491–6.
- Ohmori O, Shinkai T, Kojima H, Terao T, Suzuki T, Mita T, *et al.* Association study of a functional catechol-O-methyltransferase gene polymorphism in Japanese schizophrenics. *Neurosci Lett* 1998; 243: 109–12.
- Okubo Y, Saijo T, Oda K. A review of MRI studies of progressive brain changes in schizophrenia. *J Med Dent Sci* 2001; 48: 61–7.
- Palmatier MA, Kang AM, Kidd KK. Global variation in the frequencies of functionally different catechol-O-methyltransferase alleles. *Biol Psychiatry* 1999; 46: 557–67.
- Paus T. Primate anterior cingulate cortex: where motor control, drive and cognition interface. *Nat Rev Neurosci* 2001; 2: 417–24.
- Pezawas L, Verchinski BA, Mattay VS, Callicott JH, Kolachana BS, Straub RE, *et al.* The brain-derived neurotrophic factor val66met polymorphism and variation in human cortical morphology. *J Neurosci* 2004; 24: 10099–102.
- Selemon LD. Regionally diverse cortical pathology in schizophrenia: clues to the etiology of the disease. *Schizophr Bull* 2001; 27: 349–77.
- Shenton ME, Dickey CC, Frumin M, McCarley RW. A review of MRI findings in schizophrenia. *Schizophr Res* 2001; 49: 1–52.
- Steel RM, Whalley HC, Miller P, Best J, Johnstone EC, Lawrie SM. Structural MRI of the brain in presumed carriers of genes for schizophrenia, their affected and unaffected siblings. *J Neurol Neurosurg Psychiatry* 2002; 72: 455–8.
- Stefanis NC, Van Os J, Avramopoulos D, Smyrnis N, Evdokimidis I, Hantoumi I, *et al.* Variation in catechol-O-methyltransferase val158 met genotype associated with schizotypy but not cognition: a population study in 543 young men. *Biol Psychiatry* 2004; 56: 510–5.
- Sullivan PF, Kendler KS, Neale MC. Schizophrenia as a complex trait: evidence from a meta-analysis of twin studies. *Arch Gen Psychiatry* 2003; 60: 1187–92.
- Takahashi T, Suzuki M, Hagino H, Zhou SY, Kawasaki Y, Nohara S, *et al.* Bilateral volume reduction of the insular cortex in patients with schizophrenia: a volumetric MRI study. *Psychiatry Res* 2004; 132: 187–96.
- Talairach J, Tournoux P. A coplanar stereotaxic atlas of a human brain. Three-dimensional proportional system: an approach to cerebral imaging. Stuttgart: Thieme; 1988.
- Tunbridge EM, Bannerman DM, Sharp T, Harrison PJ. Catechol-O-methyltransferase inhibition improves set-shifting performance and elevates stimulated dopamine release in the rat prefrontal cortex. *J Neurosci* 2004; 24: 5331–5.
- Weinberger DR, Egan MF, Bertolino A, Callicott JH, Mattay VS, Lipska BK, *et al.* Prefrontal neurons and the genetics of schizophrenia. *Biol Psychiatry* 2001; 50: 825–44.
- Wright IC, McGuire PK, Poline JB, Traverso JM, Murray RM, Frith CD, *et al.* A voxel-based method for the statistical analysis of gray and white matter density applied to schizophrenia. *Neuroimage* 1995; 2: 244–52.
- Yamasue H, Iwanami A, Hirayasu Y, Yamada H, Abe O, Kuroki N, *et al.* Localized volume reduction in prefrontal, temporo limbic, and paralimbic regions in schizophrenia: an MRI parcellation study. *Psychiatry Res* 2004; 131: 195–207.

Estimation of oxygen metabolism in a rat model of permanent ischemia using positron emission tomography with injectable $^{15}\text{O-O}_2$

Takashi Temma¹, Yasuhiro Magata², Yuji Kuge¹, Sayaka Shimonaka¹, Kohei Sano¹, Yumiko Katada¹, Hidekazu Kawashima³, Takahiro Mukai³, Hiroshi Watabe⁴, Hidehiro Iida⁴ and Hideo Saji¹

¹Department of Patho-Functional Bioanalysis, Graduate School of Pharmaceutical Sciences, Kyoto University, Kyoto, Japan; ²Laboratory of Genome Bio-Photonics, Photon Medical Research Center, Hamamatsu University School of Medicine, Hamamatsu, Japan; ³Department of Nuclear Medicine and Diagnostic Imaging, Graduate School of Medicine, Kyoto University, Kyoto, Japan; ⁴Department of Investigative Radiology, National Cardiovascular Center Research Institute, Suita, Japan

The threshold of cerebral blood flow (CBF) into infarction in rats has been indicated to be similar to that in patients. However, CBF does not reflect metabolic function, and so estimations of oxygen metabolism have been required. Here, we estimated changes in oxygen metabolism after occluding the right middle cerebral artery (MCA) in rats using an injectable $^{15}\text{O-O}_2$ we developed. A decrease in CBF (left: 0.67 ± 0.22 mL/min/g, right: 0.44 ± 0.17 mL/min/g, $P < 0.05$) and compensatory increase in the oxygen extraction fraction (OEF) (left: 0.42 ± 0.13 , right: 0.50 ± 0.19 , $P < 0.05$) were observed at 1-h after occlusion. In contrast, a marked decrease in CBF and the cerebral metabolic rate for oxygen and a collapse of the compensatory OEF mechanism were found at 24 h after occlusion. Injectable $^{15}\text{O-O}_2$ could be used to reliably estimate oxygen metabolism in an infarction rat model with positron emission tomography.

Journal of Cerebral Blood Flow & Metabolism advance online publication, 22 March 2006; doi:10.1038/sj.jcbfm.9600302

Keywords: OEF; oxygen metabolism; permanent ischemia; positron emission tomography; rat

Introduction

Stroke is closely related to alterations in cerebral blood flow (CBF), the cerebral metabolic rate for oxygen (CMRO₂), the oxygen extraction fraction (OEF), cerebral blood volume, and so on while some neurodegenerative disorders such as Alzheimer's disease and Parkinson's disease are also reported to induce a change in CBF (Derejko *et al*, 2001; Mori,

2002) because of tissue degradation. Therefore, estimation of these circulatory and metabolic parameters is important for both pathophysiological studies and the development or evaluation of new methods for treating stroke.

Studies on changes in parameters of cerebral circulation after the onset of stroke have been performed in several animal models (Belayev *et al*, 1997; Ginsberg, 2003; Heiss *et al*, 1997, 1994; Pappata *et al*, 1993; Takamatsu *et al*, 2000; Tenjin *et al*, 1992; Young *et al*, 1996; Zhao *et al*, 1997) and patients (Baron, 2001; Heiss *et al*, 2001). In the studies using larger animals, CBF, OEF and CMRO₂ were estimated after the onset of ischemia by positron emission tomography (PET) with $^{15}\text{O-H}_2\text{O}$ and $^{15}\text{O-O}_2$ gas and used as predictors for the progression of brain infarction. These reports indicated that areas showing a decrease in CBF and compensatory increase in OEF in the early phase of stroke were vital several hours after the onset. Also, in studies with rats as an animal model of ischemia, CBF was certainly indicated to be a good predictor for infarction in comparison with the results for

Correspondence: Dr Y Magata, Laboratory of Genome Bio-Photonics, Photon Medical Research Center, Hamamatsu University School of Medicine, 1-20-1 Handayama, Hamamatsu 431-3192, Japan.

E-mail: magata@hama-med.ac.jp

This study was partly supported by Mitsubishi Pharma Research Foundation. This work was also supported by Grants-in-Aid for Scientific Research and by the 21st Century Center of Excellence Program at Kyoto University 'Knowledge Information Infrastructure for Genome Science' and at Hamamatsu University School of Medicine 'Medical Photonics' from the Ministry of Education, Culture, Sports, Science and Technology, Japan.

Received 4 October 2005; revised 7 February 2006; accepted 10 February 2006

patients (Belayev *et al*, 1997; Ginsberg, 2003; Zhao *et al*, 1997). However, CBF does not reflect cell energy metabolism and so measurements of oxygen metabolism are required to accurately estimate tissue viability. Additionally, since that there are functional differences between rodents and humans (Walovitch *et al*, 1994), careful evaluation is needed when using rats to investigate the pathophysiology and progression of human stroke. On these bases, we adopted MCA occluded rats, widely used ischemia model (Kuge *et al*, 1995; Longa *et al*, 1989; Minematsu *et al*, 1992), and evaluated the changes in CBF, OEF and CMRO₂ after the onset of stroke with PET.

On the other hand we recently developed a method of measuring regional OEF in the rat brain noninvasively using PET (Magata *et al*, 2003). Here, we designed experiments to estimate CBF, OEF and CMRO₂ by PET in the early and late phases of a permanent ischemia in rats.

Materials and methods

Animals

Male Sprague–Dawley rats (250 to 310 g) supplied by Japan SLC Co. (Hamamatsu, Japan) were housed for 1 week under a 12-h light/12-h dark cycle and given free access to food and water. The animal experiments in this study were conducted in accordance with institutional guidelines and approved by the Kyoto University Animal Care Committee.

Preparation of ¹⁵O-Labeled Compounds

The production of ¹⁵O-H₂O and injection of ¹⁵O-oxygen (injectable ¹⁵O-O₂) were conducted as reported previously (Magata *et al*, 2003). Briefly, ¹⁵O-H₂O was synthesized by the reduction of ¹⁵O-O₂ with H₂ gas (catalyzed by Pd black at 140°C) and trapped in a saline solution. As for injectable ¹⁵O-O₂, part of an infusion line kit (Terumo Corporation, Tokyo, Japan) used as a blood reservoir and an artificial lung 18 cm in length (Senko Medical Instrument Mfg Co. Ltd, Tokyo, Japan) designed for small animals such as rats were connected to a peristaltic pump (EYELA roller pump RP-1000, Tokyo Rikakikai Co. Ltd, Tokyo, Japan) to make a closed system. Then, 18 to 20 mL of blood was collected from several rats and filtered with saline-wetted gauze. The blood was circulated (100 mL/min) in the system and ¹⁵O-O₂ gas (4100 to 5100 MBq/min/500 ml) was introduced into the artificial lung to prepare injectable ¹⁵O-O₂ (51 to 90 MBq/ml).

Animal Preparation

Rats were divided into two groups. One was for the early phase PET experiment ($n=7$, 1 h after the onset of occlusion) and the other was for the late phase experiment ($n=6$, 24 h after the onset of occlusion). The rats were starved for 6 h before the operation and anesthetized with

chloral hydrate (i.p. 400 mg/kg). For the early phase group, anesthesia was sustained throughout the experiment. The left femoral artery in each rat was catheterized using a PE 20 catheter (i.d. 0.5 mm, o.d. 0.8 mm) for blood sampling during PET study. Then, the right middle cerebral artery (MCA) was occluded intraluminally using a nylon 4-0 monofilament (Kuge *et al*, 1995; Longa *et al*, 1989; Minematsu *et al*, 1992). For the late phase group, each rat was aroused from anesthesia after the right MCA occlusion and then anesthetized for the catheterization of the left femoral artery and PET experiments. After the completion of the operation, rats were administered i.v. with 100 IU of heparin. The animal was placed supine in a stereotaxic apparatus, and its head was restrained by mouth and ear bars. After the acquisition of a blank scan for 180 mins, the apparatus was placed in a PET camera (SHR-7700L, Hamamatsu Photonics, Hamamatsu, Japan) (Watanabe *et al*, 1997). The position was standardized with the aid of a laser beam, and the desired cranial position in the camera was oriented. Rectal temperature was maintained at around 37 °C with the aid of heating pads and blood gases were measured using a blood gas analyzer (Rapidlab 348, Chiron Diagnostics Ltd, Essex, England) several times during the experiment. After the PET experiments, 2,3,5-triphenyltetrazolium chloride (TTC) staining was performed in some cases for evaluating the progression of stroke.

Positron Emission Tomography Experiments

A transmission scan was performed for 30 mins for attenuation correction following the blank scan. Then, a dynamic PET scan was performed using ¹⁵O-H₂O (i.v., 148 to 185 MBq) to measure CBF values 1 h or 24 h after the initiation of MCA occlusion. A second PET scan was performed with the administration of injectable ¹⁵O-O₂ (i.v., 74 to 148 MBq) over a 60-secs period to measure OEF values after the radioactivity of ¹⁵O-H₂O had decayed in the body. In both cases, the total scan acquisition period was 120 secs and the scan consisted of 12 × 10-second frames. Arterial blood sampling was performed continuously throughout the PET scans and blood centrifugation was also performed for measuring the plasma concentration of ¹⁵O radioactivity. The radioactivity of each sample was measured with a NaI well scintillation counter (Packard AutoGamma 500, Packard Instruments, Meriden, CT, USA) calibrated using a ²²Na standard radioactive source.

Data Analysis

Positron emission tomography images were obtained as described previously (Magata *et al*, 2003). The rat brain was visualized in four consecutive coronal slices. Then, two regions of interest (ROIs) in each slice, right and left hemispheres, were visually chosen according to the magnetic resonance images obtained previously in the another study using 1.5T MRI. Activity in ROIs was calibrated using a cross calibration factor calculated in

another phantom study with a 10-cm-diameter hollow phantom.

The CBF value in each ROI was calculated by numerically solving the equation (1) as reported previously (Temma *et al*, 2004).

$$R(t) = fA_w(t) * e^{-(f/p+\lambda)t} \quad (1)$$

where the asterisk denotes the convolution integral and other marks are the tissue concentration of ^{15}O radioactivity ($R(t)$), a typical example of that in the late phase experiment is presented in Figure 1, CBF (f), the arterial concentration of ^{15}O -water radioactivity ($A_w(t)$), partition coefficient of water between the brain and blood ($P=0.8$) and physical decay constant of ^{15}O (λ).

Then, the OEF value was calculated using the same equation (Eq. 2) as that applied to the bolus inhalation of ^{15}O - O_2 gas method (Mintun *et al*, 1984; Shidahara *et al*, 2002), which could be used with this pharmaceutical as shown previously (Magata *et al*, 2003)

$$R(t) = \text{OEF}fA_o(t) * e^{-(f/p+\lambda)t} + fA_w(t) * e^{-(f/p+\lambda)t} + V_B R(1 - V'_V \text{OEF})A_o(t) \quad (2)$$

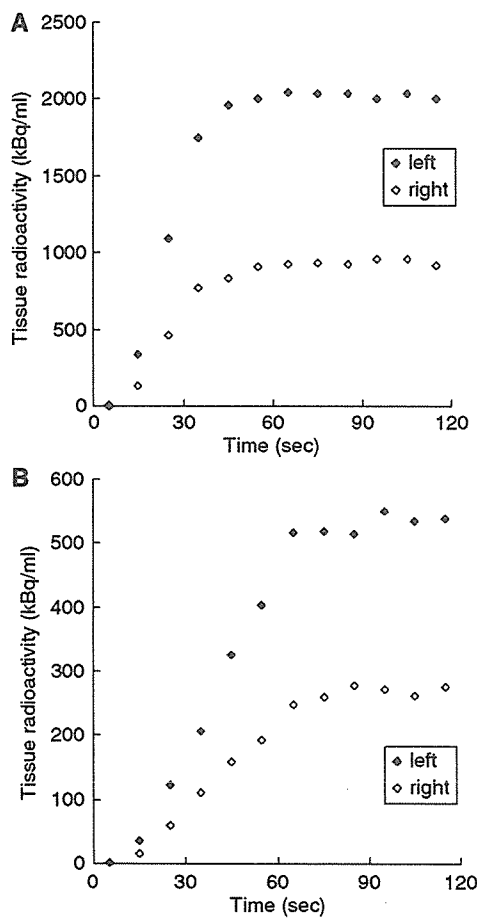


Figure 1 Typical curves of ^{15}O radioactivity obtained by the PET scanning using (A) ^{15}O - H_2O and (B) injectable ^{15}O - O_2 24 h after the right MCA occlusion.

where the arterial concentration of ^{15}O - O_2 radioactivity ($A_o(t)$), cerebral blood volume ($V_B=0.04$ mL/g), the hematocrit ratio between central and peripheral regions ($R=0.85$) and the effective venous ratio in the brain ($V'_V=0.835$) are used.

The CMRO_2 value was calculated using equation (3). In this equation, Hb is gram hemoglobin/mL blood and %Sat is percent saturation of O_2 (Shidahara *et al*, 2002).

$$\text{CMRO}_2 = \frac{(1.39 \times \text{Hb} \times \% \text{Sat})}{100} \times \text{OEF} \times \text{CBF} \quad (3)$$

Results

Injectable ^{15}O - O_2 Labeling

The shape of an artificial lung was modified to increase ^{15}O labeling efficiency. Namely, the artificial lung used was three times longer (18 cm) than the previous version while the density of plastic fibers and diameter of the lung were unchanged (Magata *et al*, 2003). In this system, 90 MBq/ml was obtained at maximum.

Physiological Parameters

Blood gases were analyzed several times during the experiment (Table 1). Although several parameters were significantly changed, these changes were slight and levels were not in the abnormal range.

Studies at 1 h After Onset

The relationships between CBF, OEF and CMRO_2 at 1 h after the occlusion are shown in scatter diagrams (Figures 2 and 3). As revealed in Figure 2, in the right hemisphere, a decrease in CBF and compensatory increase in OEF were indicated in comparison with the opposite side, inducing a good reciprocal relationship as a whole. Also, the decrease in CBF in the right hemisphere was not so marked. Figure 3 shows the relationship between CBF and CMRO_2 .

Table 1 Arterial blood gas values before and after PET experiments in MCA occlusion

	1 h		24 h	
	Before	After	Before	After
pH	7.32 (0.03)	7.33 (0.03)	7.36 (0.04)	7.35 (0.04)
PO_2 (mm Hg)	97.4 (5.7)	102.8 (10)	94.8 (7.4)	101.5 (4.3)*
PCO_2 (mm Hg)	44.3 (4.2)	39.8 (3.4)	39.7 (4.8)	36.9 (3.7)*
Hct (%)	54.4 (4.8)	51.5 (3.8)*	55 (3.3)	53.5 (3.1)
O_2Sat (%)	96.9 (0.4)	97.2 (0.8)	96.9 (0.7)	97.4 (0.3)*
Hb (g/dl)	18.5 (1.6)	17.5 (1.3)*	18.7 (1.2)	18.2 (1.0)

Statistical differences in each physiological parameter between before and after PET experiments were determined using the Wilcoxon signed-rank test; * $P < 0.05$.

Values listed are means (s.d.).

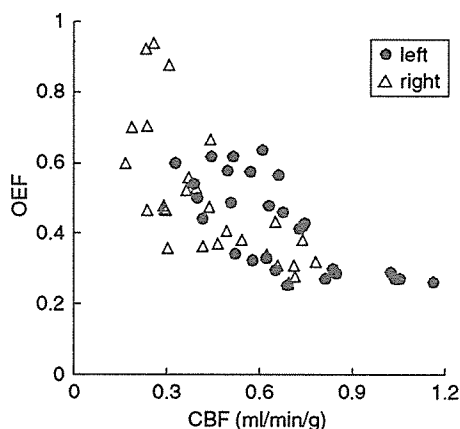


Figure 2 Scatter diagram of CBF (mL/min/g) and OEF values 1 h after the onset of MCA occlusion.

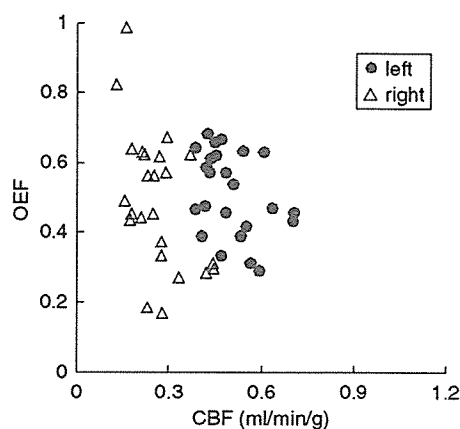


Figure 4 Scatter diagram of CBF (mL/min/g) and OEF values 24 h after the onset of MCA occlusion.

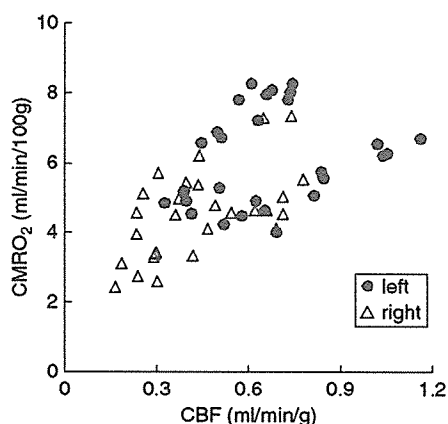


Figure 3 Scatter diagram of CBF (mL/min/g) and CMRO₂ (mL/min/100g) values 1 h after the onset of MCA occlusion.

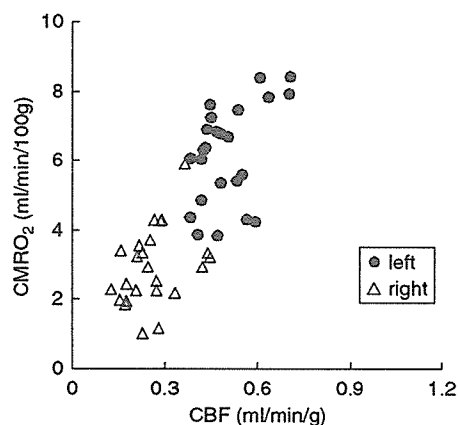


Figure 5 Scatter diagram of CBF (mL/min/g) and CMRO₂ (mL/min/100g) values 24 h after the onset of MCA occlusion.

These two values also exhibit a good correlation, in which the decrease in CMRO₂ in the right hemisphere was not so marked.

Studies at 24 h After Onset

The relationships among parameters at 24 h after the occlusion are shown in scatter diagrams (Figures 4 and 5). As shown in Figure 4, in the right hemisphere, the decrease in CBF was more pronounced than at 1 h (Figure 2) and there was no compensatory increase in OEF, resulting in a loss of the good correlation between CBF and OEF. Figure 5 shows the relationship between CBF and CMRO₂. The right hemisphere exhibited a marked decrease in CMRO₂.

Quantitative Values of Cerebral Blood Flow, Oxygen Extraction Fraction and Cerebral Metabolic Rate for Oxygen

Figure 6 and Table 2 show the averaged hemispheric values of CBF, OEF and CMRO₂ at 1 h ($n=7$) and

24 h ($n=6$) after the onset of MCA occlusion. In the right hemisphere at 1 h, the decrease in CBF was not so marked (0.44 ± 0.17 mL/min/g; $P < 0.05$ compared with the left side) and a compensatory increase in OEF (0.50 ± 0.19 ; $P < 0.05$ compared with the left side) was observed, inducing a slight decrease in CMRO₂ (4.5 ± 1.1 mL/min/100g; $P < 0.05$ compared with the left side). In contrast, at 24 h, there was a marked decrease in CBF (0.26 ± 0.07 mL/min/g, $P < 0.05$ compared with both the left side and at 1 h) and no compensatory increase in OEF (0.49 ± 0.19 ; OEF in the left hemisphere was 0.51 ± 0.12 , not significant with each other), resulting in a large decrease in CMRO₂ (2.9 ± 0.8 mL/min/100g; $P < 0.05$ compared with both the left side and at 1 h).

Discussion

In our previous report (Magata *et al*, 2003), up to 72 MBq/ml of injectable ¹⁵O-O₂ was obtained with

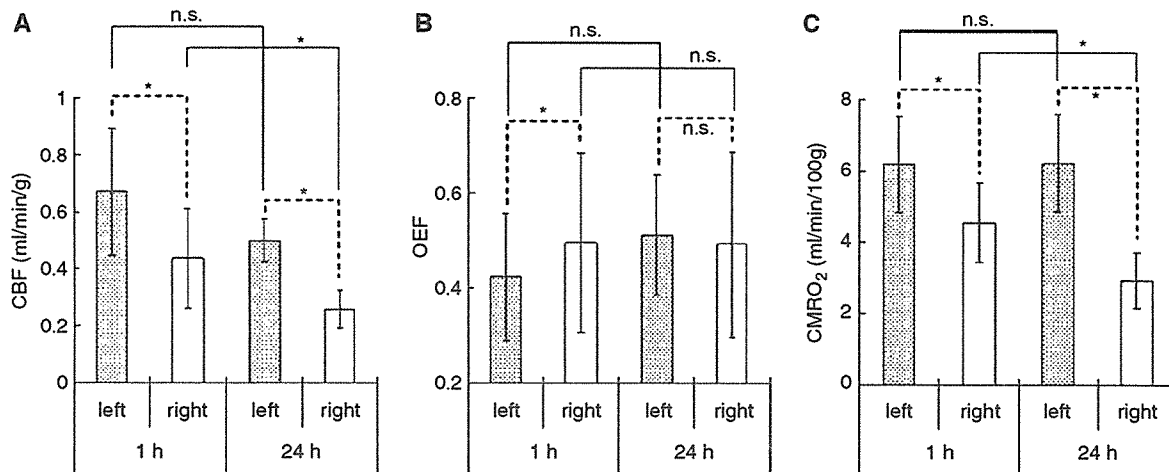


Figure 6 The averaged hemispheric values of (A) CBF (mL/min/g), (B) OEF and (C) CMRO₂ (mL/min/100 g) obtained by PET 1 (*n* = 7) and 24 h (*n* = 6) after the onset of MCA occlusion. Significant differences in each parameter (CBF, OEF, CMRO₂) between the left and right hemispheres at the same time point and between 1 h and 24 h on the same hemisphere were determined using the Wilcoxon signed-rank test and the Mann–Whitney *U*-test, respectively; **P* < 0.05, n.s. not significant.

Table 2 The averaged hemispheric values of CBF (mL/min/g), OEF and CMRO₂ (mL/min/100 g) obtained by PET 1 (*n* = 7) and 24 hours (*n* = 6) after the onset of MCA occlusion.

	1 h		24 h	
	Left	Right	Left	Right
CBF (mL/min/g)	0.67 (0.22)	0.44 (0.17)*	0.50 (0.08)	0.26 (0.07)*†
OEF	0.42 (0.13)	0.50 (0.19)*	0.51 (0.12)	0.49 (0.19)
CMRO ₂ (mL/min/100 g)	6.2 (1.3)	4.5 (1.1)*	6.2 (1.4)	2.9 (0.8)*†

Significant differences in each parameter (CBF, OEF, CMRO₂) between the left and right hemispheres at the same time point and between 1 and 24 h on the same hemisphere were determined using the Wilcoxon signed-rank test (**P* < 0.05) and the Mann–Whitney *U*-test (†*P* < 0.05), respectively. Values listed are means (s.d.).

an artificial lung (6 cm length) and about 10 ml of blood. In the present study, the artificial lung was made three times longer to increase the labeling efficiency. First, we used three small artificial lungs connected in series to improve the labeling efficiency. In that system, more blood was needed for summation of the dead volume of each lung, and, the labeling efficiency, radioactivity per unit blood volume, did not increase. Since the total activity in the labeling system is constant if the radioactivity in the supplied gas is constant, highly specific activity of injectable ¹⁵O-O₂ can be obtained when a small amount of blood is used. Therefore, the ‘long’ artificial lung can increase the specific activity of injectable ¹⁵O-O₂ owing to the small dead volume. Actually, with this new artificial lung and 18.6 ml of blood, 90 MBq/ml of injectable ¹⁵O-O₂ was obtained.

During the experiments, arterial blood gases were analyzed several times (Table 1). At both 1 and 24 h, significant changes were observed in two or three parameters. At 1 h, Hct and Hb decreased after the experiment, indicating slight hemolytic anemia. At 24 h, pO₂, pCO₂ and O₂Sat changed during the PET

scans. These values, especially pCO₂, are known to be closely related to the depth of anesthesia and so might reflect a change in the condition of the animal in PET studies. In any case, the changes of these parameters were not so marked and they might not affect the results of experiments.

At 1 h after the onset of MCA occlusion, CBF decreased slightly but significantly in the right hemisphere in comparison with the left side; some ROIs showed normal values and others showed low values (Figure 2). The OEF increased in ROIs with decreased CBF, but not in ROIs with normal CBF (Figure 2). The results indicate that the metabolic compensatory mechanism worked well at 1 h after MCAO. Cerebral metabolic rate for oxygen was also kept in the area of low CBF (Figure 3), and a good correlation between CBF and CMRO₂ with a gentle slope was obtained (Figure 3), suggesting that the compensatory mechanism was working well at this time point.

At 24 h after the onset of MCA occlusion, while all ROIs in the right hemisphere showed severely decreased CBF with small variation, OEF showed a